Neuroscience Letters 711 (2019) 134417

Contents lists available at ScienceDirect

Neuroscience Letters

journal homepage: www.elsevier.com/locate/neulet

Research article

Structural and functional abnormalities of motor endplates in rat skeletal model of myofascial trigger spots

Qing-Guang Liu[a], Qiang-Min Huang[b,*], Lin Liu[c], Thi-Tham Nguyen[d]

[a] International College of Football, Tongji University, Shanghai, China
[b] Department of Sport Rehabilitation, School of Kinesiology, Shanghai University of Sport, Shanghai, China
[c] Department of Sport and Health Science, Nanjing Sport Institute, Nanjing, China
[d] Faculty of Sport Science, Ton Duc Thang University, Ho Chi Minh City, Viet Nam

ARTICLE INFO

Keywords:
Spontaneous electrical activity
Myofascial trigger point
Motor endplate

ABSTRACT

Myofascial trigger points (MTrPs) are defined as hyperirritable spots in a palpable taut band (TB) of skeletal muscle fibers. Knowing the formation and location of MTrPs is a great help to prevent their development and inactivate existing MTrPs. This study aimed to obtain new evidence that myofascial trigger spots (MTrSs), which are similar to human MTrPs, are found in dysfunctional motor endplates by observing the morphological characteristics of muscles and changes in biochemical substances. A total of 32 male Sprague Dawley rats were randomly divided into four groups: two control groups (i.e., C1 and C2) and two model groups (i.e., M1 and M2). C1 and M1 were used for acetylcholine (ACh) content measurement, while C2 and M2 were utilized for acetylcholinesterase (AChE) staining. In the model groups, blunt striking injury was induced and eccentric exercise was applied to the left gastrocnemius for 8 weeks. After 1 month, spontaneous electrical activity(SEA), AChE optical density (OD), muscle fiber diameter, and ACh content were measured. The results showed that extensive abnormal endplate noise (aEPN), including positive neurons, fibrillation potentials, fasciculation potential, and high amplitude (endplate spikes [EPS]), is present at MTrSs in M1. Quantitative electromyography results showed that the amplitudes of aEPN and frequency of EPS in M1 were significantly higher than those of C1. The ACh content of MTrSs in M1 was significantly higher than that in C1. The AChE OD value of M2 was significantly lower than that of C2. In addition, the diameter of the muscle fibers in the AChE-stained area was longer in M2 than in C2. In conclusion, MTrSs formed at the motor endplate with a larger diameter of muscle fibers. Excessive ACh release and decreased AChE activity at MTrSs stimulated muscle action potential and muscle contraction.

1. Introduction

Myofascial trigger points (MTrPs) are defined as hyperirritable spots in a palpable taut band (TB) of skeletal muscle fibers [1]. Accordingly, puncturing or pressing MTrPs can produce local twitch responses accompanied by spontaneous pain and referred pain [2]. Needle electromyography (EMG) [3], surface EMG [4], and ultrasound imaging [5] are valuable tools used to confirm the existence of MTrPs in human subjects. MTrPs are considered common causes of pain and dysfunction in the musculoskeletal system [6–9].

Simons and Stolov [10] found isolated, large, round muscle fibers in the cross-sections of canine myofascial trigger spots (MTrSs), which are similar to human MTrPs, and numerous contraction knots in longitudinal sections [11]. Simons [12] found that the longitudinal size of these contraction knots is similar to the length of motor endplates described by Leonard et al. [13]. In subsequent studies, Simons [1] proposes that abnormal contraction knots may be initiated by the excessive release of acetylcholine (ACh) at motor endplates. The spontaneous electrical activity (SEA) founded at MTrSs implies an excessive release of ACh [14]. Acetylcholinesterase (AChE) inhibits miniature endplate potential activity by hydrolyzing ACh [15]. When AChE is inhibited, ACh is not hydrolyzed and accumulates in the synaptic cleft. Another study found contraction disks can be formed at motor endplates by blocking AChE [16]. Sarcomeres contract at neuromuscular synapses when AChE is inhibited [17,18]. The aforementioned studies indicate that MTrSs are located at the motor endplate. However, direct morphological evidence has yet to be obtained to confirm that MTrSs are found at the motor endplates. Accordingly, the ACh and AChE levels should be measured to understand the formation of MTrSs.

AChE is concentrated and retained at the neuromuscular junctions (NMJs) and used as a marker of NMJ development [19]. The position of the motor endplates can be observed through AChE staining on the

* Corresponding author at: Keyanlou 4-408, Hengren Road No. 188, Yangpu District, Shanghai, 200438, China.
E-mail address: huaqia404@aliyun.com (Q.-M. Huang).

https://doi.org/10.1016/j.neulet.2019.134417
Received 24 May 2019; Received in revised form 3 August 2019; Accepted 5 August 2019
Available online 06 August 2019
0304-3940/

basis of the enzyme histochemical method of Karnovsky and Roots [20]. The ACh levels at the motor endplates can be analyzed using an ACh enzyme-linked immunosorbent assay (ELISA) kit. Therefore, we aimed to use AChE staining to obtain direct morphological evidence that MTrSs are located at the motor endplates. Simultaneously, the ACh levels and SEA at MTrSs were examined to explain the formation of contraction knots.

2. Methods

2.1. Animal care and experimental groups

A total of 32 male adult Sprague Dawley rats (mean age = 7 weeks, weight = 220 ± 24 g) were randomly divided into four groups: two control groups (C1 and C2) and two model groups (M1 and M2). C1 and M1 were used for the ACh protein content measurement, while C2 and M2 were used for the AChE staining (morphological observation and AChE optical density test). Blunt striking injury was induced for the model rats, while eccentric exercise was applied to the left gastrocnemius muscle for 8 weeks. Thereafter, the model rats were allowed to recover for 4 weeks. The rats were housed in polypropylene cages with a 12 h/12 h light/dark cycle. The temperature and relative humidity were controlled at 20 °C–25 °C and 40%–70%, respectively. Food and water were freely provided. The individual study protocol was approved by the research ethics committee of Shanghai University of Sport (Permission No. 2014012; License No. SCXK 2007-0003).

2.2. Modeling intervention

The model rats were anesthetized by intraperitoneal (i.p.) injections (1% sodium pentobarbital, 40 mg/kg body weight) and fixed on a board thereafter using a striking device [21]. The site of the left gastrocnemius muscle was marked. The rats were hit at the marked position once a week. The hit was accomplished using a stick dropped from a height of 20 cm with a kinetic energy of 2.352 J to induce muscle contusion. On the second day of the hit, the model rats were set to run on a treadmill (DSPT-202, China) at a −16° downward angle and speed of 16 m/min for 90 min. The rats were allowed to rest for the remaining days of the week. Interventions were repeated at weekly intervals for 8 weeks, while recovery was set for 4 weeks. Accordingly, the MTrS modeling was completed.

2.3. Identification of MTrS and SEA collection

TB and MTrSs were identified through finger palpation with gentle rubbing [22] and needle EMG examination [23] after the rats were anesthetized. The SEA recordings were obtained using EMG equipment (NeuroCare-E, NCC Medical Co., LTD, Shanghai, China; sampling frequency at 50,000 Hz) with three fine needle electrodes (Φ0.3 mm). A band with a filter was set at 20 Hz to 3000 Hz, the gain was set at 20 μV/division, and the sweep speed was 10 ms/division. The ground and reference electrodes were inserted into the tail and TB, respectively, of the gastrocnemius. If a local twitch response was detected, then TB was considered a possible MTrS. For confirmation, the recording electrode was inserted longitudinally into the TB at approximately 3–5 mm away from the reference electrode. If SEA was detected, then TB was denoted an MTrS and recorded for 2 min. SEA is a combination aEPN (continuous with noise-like action potentials at 10–80 μV) and EPS (intermittent large amplitude spikes at 100–600 μV) [24–26]. The peak-to-peak value within groups was calculated. The regions where SEA was found were marked on the skin using an indelible marker.

2.4. Histological analysis

Prior to tissue sampling, all rats were euthanized by decapitation under deep anesthesia with sodium pentobarbital (50 mg/kg). The left gastrocnemius tissues (under the marked area) of the rats in C2 and M2 were rapidly dissected. The tissues were fixed by immersion in 4% paraformaldehyde diluted in 0.1 M phosphate buffer (PB, pH 7.4) at 4 °C for 12 h. The tissues were placed in 20% sucrose diluted in 0.1 M phosphate buffer (PB, pH 7.4) at 4 °C for 12 h for dehydration. Thereafter, the tissues were dried using a filter paper, embedded in an optimum cutting temperature compound in a custom-made frame, and rapidly frozen in liquid nitrogen. Tissue sections were prepared on a cryostat (Leica CM1900, Leica Microsystems, Wetzlar, Germany) with 15 mm thick transverse slices. The slices were selected from every 10 slices, and each tissue sections was selected five slices. Each slice was stained with modified Karnovsky–Roots solution [27] at 4 °C for 12 h. Thereafter, the slices were rinsed with distilled water thrice for 15 min each and air-dried. Eventually, the neutral gum was sealed. Images were obtained under an optical microscope connected to a photographic machine (Olympus DP80, Tokyo, Japan). At 200× magnification, each slice was randomly selected under a light microscope for 2 fields of view, while 80 fields were measured in each group. The diameter of muscle fibers and optical density (OD) were analyzed separately by two pathologists. The average of the obtained values was determined and the final result for each sample was expressed as a mean.

The Karnovsky–Roots incubation medium comprises 12.5 mg of acetylthiocholine iodide, 7 ml of 0.1 mol/L NaH_2PO4, 9 ml of 0.1 mol/L NaH_2PO_4, 1 ml of 0.1 mol/L sodium citrate, 2.5 ml of 30 mmol/L $CuSO_4$, 2.5 ml of 5 mmol/L potassium ferricyanide, 4 mmol/L iso-OMPA 0.5 ml, and 2 ml of double-distilled water.

2.5. ELISA

The rats in C1 and M1 were sacrificed as in Section 2.4. The tissues (100 mg) were dissected under the marked sites (MTrSs) and placed in 900 ml phosphate-buffered saline (PBS; pH 7.4). The tissues were rapidly fragmented using a pair of ophthalmic scissors and homogenized using an ultrasonic wave (10 s on and 10 s off, repeated 2–3 times) and a high-speed vibration (6000 rpm, 20 s on and 10 s off, repeated 2–3 times) device. The tissue homogenates were centrifuged at 8000 rpm at 4 °C for 10 min. Thereafter, the supernatant was extracted and stored at −80 °C. The ACh protein contents in the samples were measured using ACh ELISA kits (A21170; Westang, Shanghai, China). ACh was quantified through ELISA in accordance with the manufacturer's protocol. OD was read at 450 nm within 30 min by using a micro-plate reader (Denley Dragon Wellscan MK 3, Finland). Concentrations were calculated on the basis of the standard curve multiplied by the dilution factor (10×) with Ascent™ version 2.6 (Finland).

2.6. Statistical analysis

The mean and standard deviations of SEA, ACh, diameter of muscle fiber, and AChE OD levels were calculated. Independent *t*-test was conducted to assess the differences among the means between groups. Confidence intervals were set at 95% ($p < 0.05$) and 99% ($p < 0.01$).

3. Result

3.1. Animal behavior

The MTrSs rats exhibited lack of fur luster, reduced feeding and exercise, substantial quietness, more sensitivity to external stimuli, and more irritability compared with the control group. Their fur had no luster. When the striking part was touched, the rats in the MTrSs group showed fierce resistance.

3.2. MTrSs examination

The surface membrane on the gastrocnemius was flat, with no

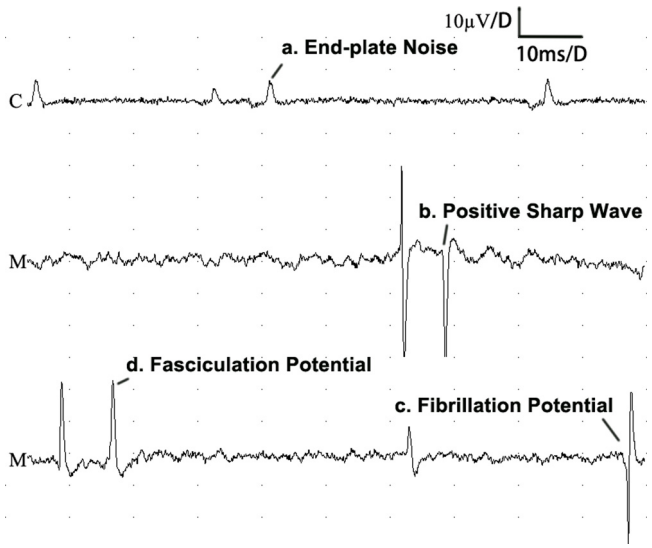

Fig. 1. EMG features between C (Control Group) and M (MTrSs Group). Normal EPN (C.a); aEPN: (M.b) Positive sharp wave starts with a positive direction, followed by a negative going wave. This wave is often present in the early stages of muscle denervation or myogenic damage; (M.c) Fibrillation potentials are triphasic, with an initial positivity followed by a long-duration negative phase; (M.d) The fasciculation potential shows a triphasic, small positive–negative–small positive potential.

tension band and contraction nodules in the control group. By contrast, the surface membrane was not flat in the MTrSs group, while TB can be touched during palpation.

3.3. EMG observations

3.3.1. aEPN

End-plate noise (EPN) is a recurring one-way negative potential with an amplitude of 10–80 μV, which is spontaneously released by ACh when end-plate is quiet and does not propagate depolarization potential. A normal EPN can be found in the control group (Fig. 1 C.a). Nevertheless, the MTrSs group has numerous different types of aEPN with characteristics of spontaneous bidirectional potentials, including positive sharp waves (Fig. 1 M.b), fibrillations (Fig. 1 M.c), and fasciculation potential (Fig. 1 M.d).

3.3.2. EPS

EPS (End-plate spike) appears intermittently, with amplitude of 100–600 μV, and the firing frequency is irregular. EPS rarely appeared in C1, but appeared continually in M1 (Fig. 2).

3.4. ACh content and SEA analysis

The quantitative EMG results showed that the amplitudes of aEPN and frequency of EPS in M1 were significantly higher than those in C1 (Table 1). The ACh content of MTrSs in M1 was significantly higher than that in C1 ($p < 0.01$) (Table 1).

3.5. Morphology observation of motor endplate and statistics

After the AChE staining, pink muscle fibers can be observed under light microscopy. The site of the motor endplate appears as a dark coffee color. At the motor endplate, the diameters of the muscle fibers in the AChE stained area were increased and the shape of AChE stained area appears as an oval-like bead in M2 (Fig. 3) but does not appear in the motor endplate of C2 ($p < 0.01$) (Fig. 3 and Table 2). This result may indicate that the structural pathological changes occurred in the motor endplate of the gastrocnemius of the model rats. This change was

Fig. 2. EPS. C1 (Control Group 1), M1 (MTrSs Group 1).

consistent with the morphological characteristics of the contraction knots of MTrSs.

AChE OD in M2 was significantly lower than that in C2 ($p < 0.05$). In addition, muscle fiber in the AChE-stained area in M2 was greater than in C2 ($p < 0.01$).

4. Discussion

This study shows for the first time the morphological nodular features of MTrSs, which are located at the motor endplates, through AChE staining. Excessive ACh release and decreased levels of AChE expression may be responsible for the formation of the contraction knots of MTrSs.

Researchers have conducted a series of studies on MTrSs in animals and humans to acquire an improved understanding of the morphological alterations of MTrSs. Simons and Stolov [10] found that MTrSs of canine gracilis muscle fibers showed a large round muscle fiber in the cross-section and a contraction knot in the longitudinal sections [11]. In the aforementioned studies, only one MTrS cell was observed in each individual field of vision. Travell and Simons [1] used the morphological features of MTrSs to make a hypothetical sketch of the MTrSs morphological features, with many contraction knots in the longitudinal section. Huang et al [21] observed several large round muscle fibers in the cross-section and a few contraction knots in the longitudinal section in each individual field of MTrSs. These observations have confirmed the assumption of the hypothetical sketch of contraction knots of MTrSs. Sikdar et al. [28] observed nodular regions through ultrasound imaging and elastography. Sarcomere contractions have been detected in biopsy [11] and fresh cadavers [29]. Simons [1,12] found that the longitudinal size of these contraction knots were extremely similar to the length of the motor endplate and hypothesized that the contraction knots of MTrSs may be located at the motor endplate. Although contraction knots have been revealed in MTrPs, previous findings cannot show whether these contraction knots were created at the endplates.

The use of the Karnovsky–Roots method for AChE staining indicated that the location of the contraction knots had deep and expanded coffee color. The AChE staining area was the site of the motor endplate [30]. This result may manifest that MTrSs are located at the motor endplate. Therefore, the AChE staining in this study showed for the first time the morphological characteristics of MTrSs that were formed at the motor endplate.

The staining area of the motor endplates in the M2 rats showed deep coffee coloring and was oval-shaped. The diameter of the muscle fibers

Table 1
ACh content and changes in the amplitudes and frequencies of aEPN and EPS.

Groups	ACh(μM/ml)	aEPN		EPS	
		Ampltudes(μV)	Frenquce(S)	Ampltudes(μV)	Frenquece(min)
C1	99.57 ± 31.02	7.91 ± 1.74	14.21 ± 3.11	177.50 ± 63.14	1.52 ± 1.64
M1	149.05 ± 35.22**	28.83 ± 5.49**	11.17 ± 2.88	162.50 ± 44.21	43.52 ± 14.72**

C1 (control group 1); M1 (MTrSs group 1); aEPN (abnormal endplate noise); EPS (end-plate potencial spikes); ACh = acetylcholine.
** $p < 0.01$, indicates a significant difference between the groups.

at the AChE staining area was larger in M2 than in C2. By contrast, this phenomenon did not occur in C2. This result corresponds to the contraction knots of MTrSs that were observed in canine gracilis muscle [31] and fresh human cadavers [29]. The OD value of AChE in M2 was lower than that in C2, indicating that AChE expression was insufficient, resulting in excessive release of ACh could not be hydrolyzed immediately, which hindered muscle relaxation process. Contraction disks are similar to contraction knots that have also been observed by locally injecting small amounts of the AChE inhibitor [16]. The inhibition of AChE causes an increase in the ACh concentrations in the synaptic cleft and promotes the formation of contraction knots [32]. Therefore, all evidence in the present study indicates that the contraction knots of MTrSs are located at the motor endplates.

As early as 1957, Weeks and Travell [33] recorded a high-frequency repetitive spike from MTrPs of trapezius at rest, but they did not detect the EMG activities in the adjacent sites. Liley [34] identified low-amplitude continuous discharges as abnormal endplate potentials. Eventually, all those potentials were called SEA [1]. Ito et al. [35] demonstrated that SEA is attributed to the excessive release of ACh packets. In the current study, the normal potentials of EPN were found in C1, whereas numerous abnormal SEAs (apart from EPN) were found in M1. Further analysis has revealed that different types of abnormal potentials included aEPN and EPS. The amplitudes of aEPN and frequency of EPS in M1 were significantly higher than those in C1. The ACh level in M1 was higher than that in C1. Therefore, aEPN of MTrSs is related to the excessive release of ACh from the motor endplate. Botulinum toxin injection into MTrSs can reduce SEA by preventing ACh release into synaptic space, thereby supporting aEPN was form by excessive release of ACh [22]. Contraction knots may activate muscle spindles and produce EPS by pulling muscle fibers. The AChE expression level of the rats in M2 was less than that in C2. When AChE is insufficient, ACh is not hydrolyzed and accumulates in the synaptic cleft. A sustained increase of ACh in the synaptic cleft induces contraction knots [32]. Furthermore, a lower pH levels and higher calcitonin gene-related peptide (CGRP) concentrations were found in the direct environment of atvive MTrSs than in the latent MTrSs and normal tissue [36]. Low pH levels will downregulates AChE, increases the efficacy of ACh, and maintains the sarcomere contraction while high CGRP concentrations will intensifies the response to excess ACh at the nerve terminal by enhancing ACh receptor activity and synthesis [37]. CGRP also upregulates the ACh-receptors at the muscle and thereby creates more docking stations for ACh. These findings demonstrated that increased the ACh levels and decreased AChE expression levels at MTrSs may be the source of endplate electrical activities and contraction knots. Additionally, Ca^{2+} accumulation due to sustained motor unit activity has been suggested to play a causative role in the development of MTrPs [38].

Table 2
AChE OD and the diameter of the staining muscle fibers.

Groups	AChE(OD)	Numbers of staining area(per field)	Diameter of staining muscle fibers(μm)
C2	1.11 ± 0.24	14.54 ± 1.78	22.46 ± 8.14
M2	0.86 ± 0.11*	15.77 ± 3.89	33.67 ± 12.06**

C2 (control group 2); M2 (MTrSs group 2); AChE (acetylcholinesterase); OD (optical density).
*$p < 0.05$; **$p < 0.01$, indicates a significant difference between the groups.

This research support the dysfunctional endplate hypothesis of the MTrS formation [39]. Increased ACh concentrations in the cleft of the neuromuscular endplates and decreased AChE expression levels induced local contraction. This state triggered the formation of contraction knots in MTrSs of the motor endplates.

5. Conclusions

MTrSs formed at the motor endplate with muscle fibers that have larger diameters. Excessive ACh release and decreased AChE activity at MTrSs stimulated muscle SEA and muscle contraction.

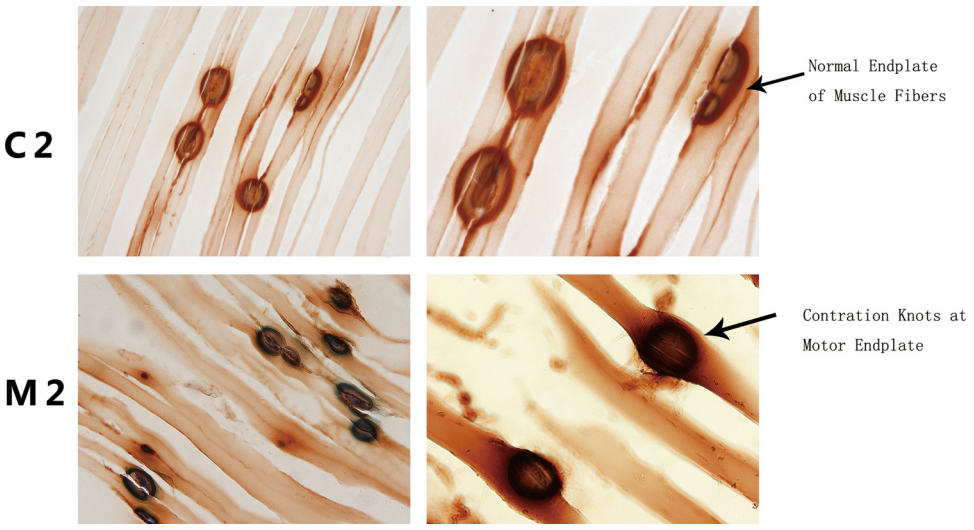

Fig. 3. AChE staining of muscle fibers: The site of the motor endplate appears as a dark coffee color after the AChE staining. At 200× magnification of the left side, the muscle fibers in C2 were straight and smooth, whereas those in M2 were curved. In the enlarged view of 400× magnification, bead-shaped contraction knots at coarsening motor endplates were found in M2, while the motor endplates in C2 were normal.

Funding

The present study is supported by the National Natural Science Foundation of China (NSFC), (grant number: 81470105).

Declaration of Competing Interest

The authors declare that there is no conflict of interests regarding the publication of this paper.

References

[1] D.G. Simons, J.G. Travell, L.S. Simons, 2nd ed., MYofascial Pain and Dysfunction: The Trigger Point Manual. Upper Half of Body Vol. 1 Williams & Wilkins, Baltimore, 1999.
[2] R.N. Harden, S.P. Bruehl, S. Gass, C. Niemiec, B. Barbick, Signs and symptoms of the myofascial pain syndrome: a national survey of pain management providers, Clin. J. Pain 16 (2000) 64–72 (Accessed 7 February 2017), http://www.ncbi.nlm.nih.gov/pubmed/10741820.
[3] D.R. Hubbard, G.M. Berkoff, Myofascial trigger points show spontaneous needle EMG activity, Spine (Phila. Pa. 1976) 18 (1993) 1803–1807, https://doi.org/10.1097/00007632-199310000-00015.
[4] D.L. Donaldson, C.C.S. Skubick, R.G. Clasby, J.R. Cram, The evaluation of trigger-point activity using dynamic EMG techniques, Am J Pain Manag. 4 (1994) 118–122.
[5] R.D. Gerwin, D. Duranleau, Ultrasound identification of the myofacial trigger point, Muscle Nerve 20 (1997) 767–768 (Accessed 23 February 2017), http://www.ncbi.nlm.nih.gov/pubmed/9149092.
[6] S.A. Skootsky, B. Jaeger, R.K. Oye, Prevalence of myofascial pain in general internal medicine practice, West. J. Med. 151 (1989) 157–160 http://www.ncbi.nlm.nih.gov/pubmed/2788962%5Cnhttp://www.pubmedcentral.nih.gov/articlerender.fcgi?artid=PMC1026905.
[7] D.G. Simons, Review of enigmatic MTrPs as a common cause of enigmatic musculoskeletal pain and dysfunction, J. Electromyogr. Kinesiol. 14 (2004) 95–107, https://doi.org/10.1016/j.jelekin.2003.09.018.
[8] D.J. Alvarez, P.G. Rockwell, Trigger points: diagnosis and management, Am. Fam. Physician 65 (2002) 653–660, https://doi.org/10.1016/j.jpowsour.2014.05.101.
[9] G.A. Malanga, E.J. Cruz Colon, Myofascial low back pain: a review, Phys. Med. Rehabil. Clin. N. Am. 21 (2010) 711–724, https://doi.org/10.1016/j.pmr.2010.07.003.
[10] D.G. Simons, W.C. Stolov, Microscopic features and transient contraction of palpable bands in canine muscle, Am. J. Phys. Med. 55 (1976) 65–88 (Accessed 23 February 2017), http://www.ncbi.nlm.nih.gov/pubmed/1266956.
[11] A. Reitinger, H. Radner, H. Tilscher, M. Hanna, A. Windisch, W. Feigl, Morphologische Untersuchung an Trigger punkten, Anglo. Med. Rev. 34 (1996) 256–262.
[12] D.G. Simons, Diagnostic criteria of myofascial pain caused by trigger points, J. Musculoskelet. Pain 7 (1999) 111–120, https://doi.org/10.1300/J094v07n01_11.
[13] J.P. Leonard, M.M. Salpeter, Agonist-induced myopathy at the neuromuscular junction is mediated by calcium, J. Cell Biol. 82 (1979) 811–819, https://doi.org/10.1083/jcb.82.3.811.
[14] D.G. Simons, C.-Z. Hong, L.S. Simons, Endplate potentials are common to midfiber myofacial trigger points, Am. J. Phys. Med. Rehabil. 81 (2002) 212–222, https://doi.org/10.1097/00002060-200203000-00010.
[15] D.M. Quinn, Acetylcholinesterase: enzyme structure, reaction dynamics, and virtual transition states, Chem. Rev. 87 (1987) 955–979, https://doi.org/10.1021/cr00081a005.
[16] S. Mense, D.G. Simons, U. Hoheisel, B. Quenzer, Lesions of rat skeletal muscle after local block of acetylcholinesterase and neuromuscular stimulation, J. Appl. Physiol. 94 (2003) 2494–2501, https://doi.org/10.1152/japplphysiol.00727.2002.
[17] M.J. Duxson, G. Vrbová, Inhibition of acetylcholinesterase accelerates axon terminal withdrawal at the developing rat neuromuscular junction, J. Neurocytol. 14 (1985) 337–363, https://doi.org/10.1007/BF01217751.
[18] T.N. Tiedt, E.X. Albuquerque, C.S. Hudson, J.E. Rash, Neostigmine-induced alterations at the mammalian neuromuscular junction. I. Muscle contraction and electrophysiology, J. Pharmacol. Exp. Ther. 205 (1978) 326–339.
[19] J. Massoulié, L. Pezzementi, S. Bon, E. Krejci, F.M. Vallette, Molecular and cellular biology of cholinesterases, Prog. Neurobiol. 41 (1993) 31–91, https://doi.org/10.1016/0301-0082(93)90040-Y.
[20] M.J. Karnovsky, L. Roots, A "direct-coloring" thiocholine method for cholinesterases, J. Histochem. Cytochem. 12 (1964) 219–221, https://doi.org/10.1177/12.3.219.
[21] Q.-M. Huang, G. Ye, Z.-Y. Zhao, J.-J. Lv, L. Tang, Myoelectrical activity and muscle morphology in a rat model of myofascial trigger points induced by blunt trauma to the vastus medialis, Acupunct. Med. 31 (2013) 65–73, https://doi.org/10.1136/acupmed-2012-010129.
[22] T.-S. Kuan, J.-T. Chen, S.-M. Chen, C.-H. Chien, C.-Z. Hong, Effect of botulinum toxin on endplate noise in myofascial trigger spots of rabbit skeletal muscle, Am. J. Phys. Med. Rehabil. 81 (2002) 512–520, https://doi.org/10.1097/00002060-200207000-00008 quiz 521–523.
[23] Q.-M. Huang, J.-J. Lv, Q.-M. Ruanshi, L. Liu, Spontaneous electrical activities at myofascial trigger points at different stages of recovery from injury in a rat model, Acupunct. Med. 33 (2015) 319–324, https://doi.org/10.1136/acupmed-2014-010666.
[24] A.W. Liley, An investigation of spontaneous activity at the neuromuscular junction of the rat, J. Physiol. 132 (1956) 650–666 http://www.pubmedcentral.nih.gov/articlerender.fcgi?artid=1363576&tool=pmcentrez&rendertype=abstract.
[25] D. Dumitru, J.C. King, D.F. Stegeman, Endplate spike morphology: a clinical and simulation study, Arch. Phys. Med. Rehabil. 79 (1998) 634–640, https://doi.org/10.1016/S0003-9993(98)90036-3.
[26] Q.G. Liu, L. Liu, Q.M. Huang, T.T. Nguyen, Y.T. Ma, J.M. Zhao, Decreased spontaneous electrical activity and acetylcholine at myofascial trigger spots after dry needling treatment: a pilot study, evidence-based complement, Altern. Med. 2017 (2017), https://doi.org/10.1155/2017/3938191.
[27] L. Li, F. Yang, X. Li, et al., Modified acetylcholinesterase staining showed rabbit skeletal muscle motor endplate, J. Clin. Exp. Pathol. 25 (2009) 218, https://doi.org/10.1109/MAP.2011.6138455.
[28] S. Sikdar, J.P. Shah, T. Gebreab, R.H. Yen, E. Gilliams, J. Danoff, L.H. Gerber, Novel applications of ultrasound technology to visualize and characterize myofascial trigger points and surrounding soft tissue, Arch. Phys. Med. Rehabil. 90 (2009) 1829–1838, https://doi.org/10.1016/j.apmr.2009.04.015.Novel.
[29] A. Windisch, A. Reitinger, H. Traxler, H. Radner, C. Neumayer, W. Feigl, W. Firbas, Morphology and histochemistry of myogelosis, Clin. Anat. 12 (1999) 266–271, https://doi.org/10.1002/(SICI)1098-2353(1999)12:4<266::AID-CA5>3.0.CO;2-G.
[30] M.A.O. Yajun, L.I. Jian, L.I. Bing, Morphological study and clinical significance of skeletal muscle's motor end plates and motor points in rabbits, Chin. J. Rehabil. Med. 26 (2011), https://doi.org/10.3969/j.issn.1001-1242.2011.11.006.
[31] D.G. Simons, W.C. Stolov, Microscopic features and transient contraction of palpable bands in canine muscle, Am. J. Phys. Med. 55 (1976) 65–88 http://www.ncbi.nlm.nih.gov/pubmed/1266956.
[32] R. Margalef, M. Sisquella, M. Bosque, C. Romeu, O. Mayoral, S. Monterde, M. Priego, R. Guerra-Perez, N. Ortiz, J. Tomas, M.M. Santafe, Experimental myofascial trigger point creation in rodents, J. Appl. Physiol. 126 (2019) 160–169, https://doi.org/10.1152/japplphysiol.00248.2018 japplphysiol.00248.2018.
[33] V.D. Weeks, J.G. Travell, How to give painless injections, A.M.A. Sci. Exhib. (Grune Strat. New York) (1957) 318–322.
[34] A.W. Liley, An investigation of spontaneous activity at the neuromuscular junction of the rat, J. Physiol. 132 (1956) 650–666 http://www.pubmedcentral.nih.gov/articlerender.fcgi?artid=1363576&tool=pmcentrez&rendertype=abstract.
[35] Y. Ito, R. Miledi, A. Vincent, Transmitter release induced by a "factor" in rabbit serum, Proc. R. Soc. London. Ser. B, Biol. Sci. 187 (1974) 235–241 (Accessed 8 March 2017), http://www.ncbi.nlm.nih.gov/pubmed/4154012.
[36] J.P. Shah, E.A. Gilliams, Uncovering the biochemical milieu of myofascial trigger points using in vivo microdialysis: an application of muscle pain concepts to myofascial pain syndrome, J. Bodyw. Mov. Ther. 12 (2008) 371–384, https://doi.org/10.1016/j.jbmt.2008.06.006.
[37] C. Bron, J.D. Dommerholt, Etiology of myofascial trigger points, Curr. Pain Headache Rep. 16 (2012) 439–444, https://doi.org/10.1007/s11916-012-0289-4.
[38] H. Gissel, T. Clausen, Excitation-induced Ca2+ influx and skeletal muscle cell damage, Acta Physiol. Scand. 171 (2001) 327–334, https://doi.org/10.1046/j.1365-201X.2001.00835.x.
[39] D.G. Simons, Clinical and etiological update of myofascial pain from trigger points, J. Musculoskelet. Pain 4 (1996) 93–121, https://doi.org/10.1300/J094v04n01_07.